Paper submitted to 6th Topical Meeting on the Technology of Fusion Energy, San Francisco, March 3-7, 1985.

STRUCTURAL RESPONSES TO PLASMA DISRUPTIONS IN TOROIDAL SHELLS[a]

M. S. Tillack,[b] M. S. Kazimi, L. M. Lidsky
Massachusetts Institute of Technology
Cambridge, MA

DRAFT
Submitted February 1985

[a]work supported by U.S. Department of Energy under contract DE-AP07-79ID00019.
[b]current address: University of California, Los Angeles, California

STRUCTURAL RESPONSES TO PLASMA DISRUPTIONS IN TOROIDAL SHELLS[a]

M. S. Tillack[b], M. S. Kazimi, and L. M. Lidsky
Massachusetts Institute of Technology
77 Massachusetts Avenue
Cambridge, Massachusetts 02139
(617) 253-4206

ABSTRACT

The induced pressures, stresses and strains in unrestrained axisymmetric toroidal shells are studied to scope the behavior of tokamak first walls during plasma disruptions. The modeling includes a circuit analog representation of the shell to solve for induced currents and pressures, and a separate quasi-static 1-D finite element solution for the mechanical response.

This work demonstrates that the stresses in tokamkak first walls due to plasma disruption may be large, but to first order will not cause failure in the bulk structure. However, stress concentrations at structural supports and discontinuities together with resonant effects can result in large enhancements of the stresses, which could contribute to plastic deformation or failure when added to the already large steady state thermal and pressure loading of the first wall.

INTRODUCTION

Major plasma disruptions affect first wall/blanket design and limit the first wall lifetime. The effects of disruptions can be classified into two very different categories: (1) particle and radiation loads, which induce thermal strains, erosion, changes in surface properties, etc., and (2) electromagnetic forces resulting from the rapid termination of plasma current. This paper describes the general response of the first wall to electromagnetic loading only.

The analysis presented here of the first wall electromagnetic response includes a numerical solution for induced currents, electromagnetic pressures, and pressure stresses.[1] The currents and pressures are obtained using a toroidally symmetric model with 1-D currents and 2-D fields. The plasma current is approximated by a single filament located inside the torus, with an exponential decay after t=0. This modelling is crude, but the exact details of the current profile evolution are not well known.

The calculation also includes a treatment of the structural response, including displacements, stresses, and strains. This part of the problem is 1-D in the poloidal angle, using toroidal axisymmetry. Most of the spatial details are ignored in order to simplify the analysis. Consequently, design variations can be easily analyzed and compared. In this work, variations in aspect ratio, plasma current, plasma shift, vertical magnetic field, and several other design variables are studied.

In addition to the static response to disruption loading, resonant behavior of toroidal shells were studied using the PAFEC finite element code. A large number of modal resonances covering a wide range of frequencies occur in tori, making resonant structural behavior an essential aspect of first wall design and analysis.

Significant differences in both the magnitude and spatial variation of loading and structural response occur when the device parameters are varied, including the allowance of a finite plasma shift. But, for all of the cases studied, the peak stresses are well below design limits. Structural discontinuities and modal resonances are a possible source of increased stresses beyond the static uniform shell case.

SURVEY OF PRESSURES AND STRESSES

Overview of Pressures

In order to compute the J×B pressures, first the induced currents must be solved. Figure 1 shows the geometry, with currents directed along θ and the magnetic field confined the the R-z plane. The structure includes a conducting toroidal shell whose volume contains the current-carrying plasma. When the plasma current experiences a transient, there are currents induced in the shell which attempt to maintain the field pattern unchanged. If the magnetic diffusion time of the torus is long compared to the transient

[a]Work supported under DOE contract DE-AP07-79ID00019.
[b]Current address: Mechanical, Aerospace & Nuclear Engineering Department, University of California, Los Angeles, California 90024, (213) 206-1230.

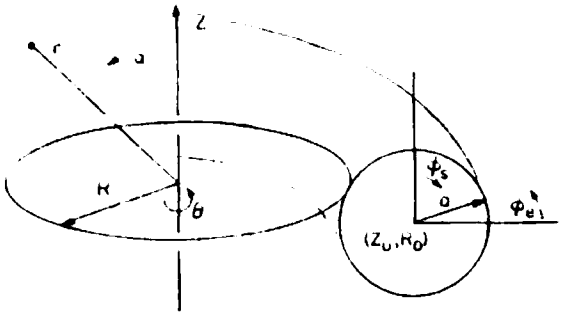

Fig. 1 Coordinate System

time constant, then the structural currents are large and decay slowly. This is generally true for the examples studied here.

For a source current at the center of the torus, the induced currents are peaked on the part of the shell closest to the major axis. This is primarily because the inner side has a lower resistance due to the shorter path. This is emphasized at early times in the transient when the outer radii are well shielded from the flux through the central hole. If the plasma current is shifted outward with respect to the shell axis, then the current profile will be altered. A shifted current example is analyzed later for comparison.

The pressures generated by a disruption can be generalized into three main components:

1. Minor radius compression. The induced currents always flow in the same direction as the plasma current. This results in a minor radius compression due to shell current interaction with both the shell current magnetic fields (self-interactions) and the plasma current magnetic fields (plasma-interactions).

2. Hoop force expansion. The hoop force attempts to expand the shell towards a larger major radius. On the inboard side it is aligned with the major radius component of the compressive force. On the outboard side the two forces tend to cancel. This is a principal source of the poloidal asymmetry observed. The plasma fields also have a hoop force effect on the shell current. Early in the disruption when the currents are peaked on the inside, the plasma current draws the shell outward away from the major axis (and the plasma current is itself drawn inward).

3. Vertical field interaction. The vertical field interaction with the shell current yields a force directed towards the torus major axis, opposite to the hoop force. Depending on the geometry, field strength, and time during the transient, the three forces become more or less dominant. The result is that in some cases there exists substantial poloidal variation of the forces but in other cases there is little. The magnitude of the vertical field is the primary cause for differences in the time evolution of the loading for different geometries. In some cases the forces are directed towards the major axis throughout most of the disruption and in other cases the inboard forces can be outwardly directed.

Since the vertical field interaction scales as I (the shell current) and the other two force scale as I^2, at sufficiently low values of current the vertical field interaction is the dominant force. This is true at the beginning and end of the current transient in the structure. This implies that near the end of the current transient when the first wall is most likely to exhibit melting at the surface, the forces tend to be directed toward the major axis. In some designs, the time at which the forces turn inward is very late in the disruption, perhaps even after the plasma current has completely vanished.

Overview of Stresses

After the pressure loading is determined, the response of the shell can be solved. Although it is substantially more complicated, the structural response of the first wall has a general behavior which can also be summarized qualitatively. One of the most interesting aspects of the stress problem in thin toroidal shells is the existence of large deformations at the top and bottom points of the poloidal cross section. The nature of the curvature at these locations results in the inapplicability of linear membrane theory, substantially complicating the analysis. This occurs even with uniform pressure loading.

Allowing non-linear response (i.e., solving the equations at the deformed points) or allowing bending moments and shears are both valid techniques to cure this problem. The method adopted here is a complete bending theory solution, accounting correctly for the generated moments and shears.

Another feature of the structural problem in a torus is the competition between major and minor radius effects. In a uniform pressure loaded problem the inboard side tends to displace less than the outboard side due to the cancellation of the hoop force and the radial pressure. In addition, strains are moderated on the inboard side due to a 1/R major radius effect:

$$R\varepsilon_\theta = v\cos\phi + w\sin\phi \qquad (1)$$

In the eddy current loaded problem, the pressures are not uniform and the strains and displacements are consequently much more complicated.

DESCRIPTION OF THE CALCULATIONS

The Eddy Current Problem

The eddy current problem is solved using an electric circuit analog of the structure. The torus is broken into a large number (typically 100) of filamentary loops coaxial to the plasma current and spaced equally along the poloidal angle. Each loop is assigned a resistance, R, and a self inductance, L:

$$R = \frac{2\pi r \eta}{h a \Delta\phi} \tag{2}$$

$$L = \frac{\mu_o}{2\pi}\left(\log\frac{8R}{a} - 1.75\right) \tag{3}$$

where $b = \sqrt{ha\Delta\phi/\pi}$

In addition, each loop couples with the plasma current and with each of the other loops through a mutual inductance. The mutual inductance is computed using the vector potential A_ϕ:

$$MI = 2\pi R A_\phi \tag{4}$$

The vector potential and the fields due to circular current loops are well known. The solution of the problem can now be obtained by solving numerically the matrix loop voltage equation:

$$M\frac{dI}{dt} + RI + M_p\frac{dI_p}{dt} = 0 \tag{5}$$

Fields are computed from the known currents, and the electromagnetic pressure is given by

$$p = hJ\times B \tag{6}$$

The Structural Problem

In the structural part of the problem, the pressures are used as input and the structural response (the stress, strain, and displacement state) is computed assuming quasi-static conditions at a given time step. The elimination of the inertial terms in the equilibrium equations is not strictly valid. In order that inertial terms can be dropped, the transient time must be long compared to the time a sound wave takes to travel across the structure, or:

$$\tau > \frac{r}{\sqrt{E/\rho}} \tag{7}$$

The characteristic time for steel structures the size of a fusion first wall is about 10 msec, compared to the disruption time of 25 msec used in this work, making the approximation questionable. Nevertheless, quasi-static response is assumed in order to simplify the analysis.

The derivation of the static structural equations follows closely the work of Flugge.[2] As shown in Ref. 1, the deformation relations are obtained by simultaneously solving the equilibrium equations subject to Hooke's law and the strain-displacement relations. The equilibrium equations are force balances in r and ϕ and a moment balance perpendicular to both r and ϕ, whereas Hooke's law relates stresses to strains. The result is

$$\sigma_\phi = \frac{D}{h}\left[\frac{1}{a}\left(\frac{dv}{d\phi} + w\right) + \frac{\nu}{r}(v\cos\phi + w\sin\phi)\right] \tag{8}$$

$$\sigma_\theta = \frac{D}{h}\left[\frac{1}{r}(v\cos\phi + w\sin\phi) + \frac{\nu}{a}\left(\frac{dv}{d\phi} + w\right)\right] \tag{9}$$

$$M_\phi = \frac{K}{a}\left[\frac{d}{d\phi}\left(\frac{1}{a}\frac{dw}{d\phi} - \frac{v}{a}\right) + \frac{\nu\cos\phi}{r}\left(\frac{dw}{d\phi} - v\right)\right] \tag{10}$$

$$M_\theta = \frac{K}{a}\left[\frac{\cos\phi}{r}\left(\frac{dw}{d\phi} - v\right) + \nu\frac{d}{d\phi}\left(\frac{1}{a}\frac{dw}{d\phi} - \frac{v}{a}\right)\right] \tag{11}$$

The bending stress, σ_b, is defined by

$$\sigma_b = \frac{6M}{h^2} \tag{12}$$

The structural equations are solved by a finite element method. The partial differential equations are translated into algebraic equations by assuming a solution in each element composed of 5th order spline functions (polynomials). Fifth order polynomials were chosen becuse of the occurence of fourth derivatives when the structural equations are combined.

The validity of the modeling was tested by comparing the results with a commercial finite element structural code, PAFEC. A uniform pressure loaded case was analyzed using 3-noded axisymmetric thin shell elements in PAFEC. Results were within 5-10%; in all likelihood the PAFEC results were less accurate, owing to the much smaller number of elements necessarily used. Figure 2 shows the displacements in a pressurized torus. The magnitude of the displacement is proportional to the distance of the dotted line from the solid circle. The high bending moments at the

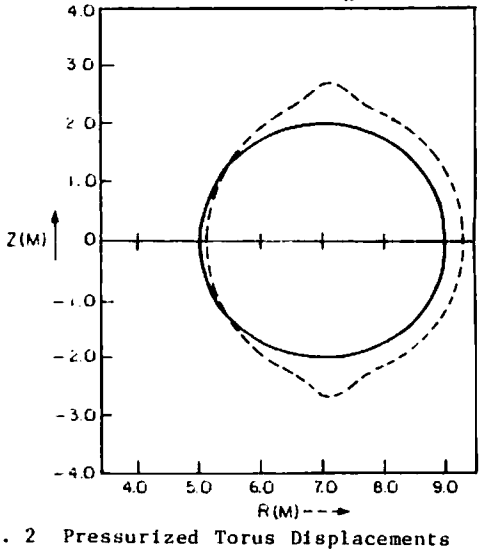

Fig. 2 Pressurized Torus Displacements

Table 1 Device Parameter Summary

device parameter	base case	high field case
minor radius (m)	2	1.24
major radius (m)	7	4.35
plasma current (MA)	10.1	8.96
toroidal field (T)	7	10
poloidal field (T)	0.35	0.50
vertical field (T)	0.067	0.067
toroidal beta (%)	2.9	2.9
poloidal beta (%)	100	1.43

top and bottom points are clearly visible.

RESULTS

Several cases were examined by varying the major device paramenters, including dimensions, field strength, plasma current, etc. For brevity, only three cases are discussed here. These include a STARFIRE base case device, a high field compact device, and a shifted plasma in the base case device. For a fair comparison of devices, all of the device parameters were scaled in order to preserve the total reactor power output and the rotational transform at the plama edge. This leads to the values shown in Table 1.

Figure 3 shows the radial pressure at the inboard edge as a function of time for the base case and the high field case. The peak pressures of 0.35-7.0 MPa occur at roughly 20 msec. At 100 msec, the competition between poloidal and toroidal effects has reversed. Figures 4 and 5 show the spatial profiles at 20 msec and 100 msec respectively. From these, the strong effect of plasma shift can be seen at early times. Most of the cases which were studied evolve towards a similar profile at long times.

Consistant with the pressures, Figure 6 shows that the structural response in the base case is dominated at early times by the minor radius compression - strongest at the inboard

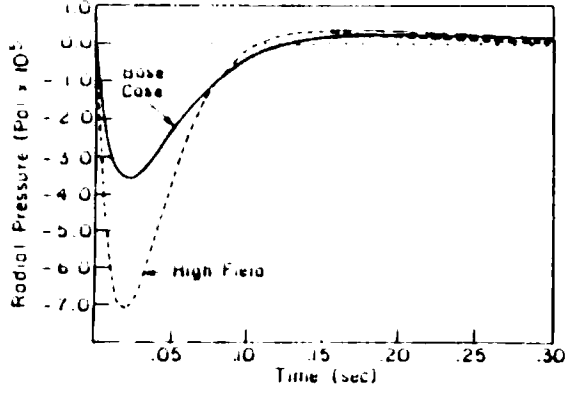

Fig. 3 Radial Pressure History at Inboard Edge

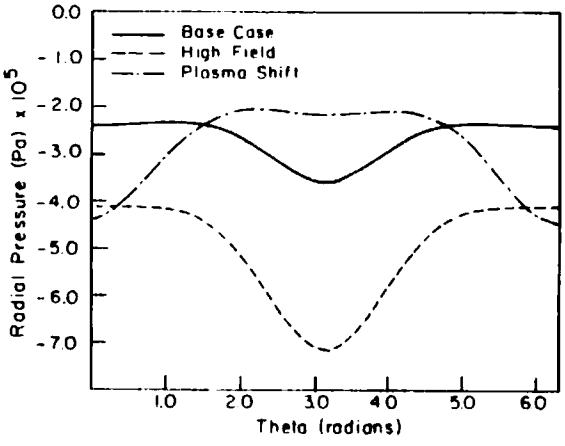

Fig. 4 Radial Pressure Profiles at 20 msec

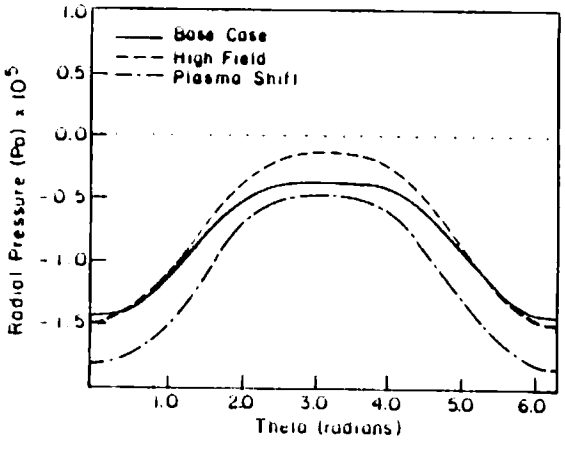

Fig. 5 Radial Pressure Profiles at 100 msec

edge. At later times (100 msec) the torus is drawn inward as the vertical field interaction becomes the dominant force. Figure 7 shows the displacements for the 25% shifted plasma, which indicates strong coupling of the plasma to the outboard part of the shell. Figures 8-9 compare the strains for the three cases.

RESONANT BEHAVIOR

Resonant vibration of reactor structures can be stimulated by impulse loading such as that due to a rapid plasma disruption. In addition, resonant periodic loading may excite resonant vibrations, for example if the plasma deforms and rotates. Resonant strains are generally larger in magnitude than nonresonant strains; if resonances exist in the structure, then it will be important to account for them in an accurate structural analysis. The vibrations of even a simple unifom torus are very complicated; due in part to the topologically connected geometry, strain resonances couple flexural, torsional, and bending energies in a way which is extremely difficult to

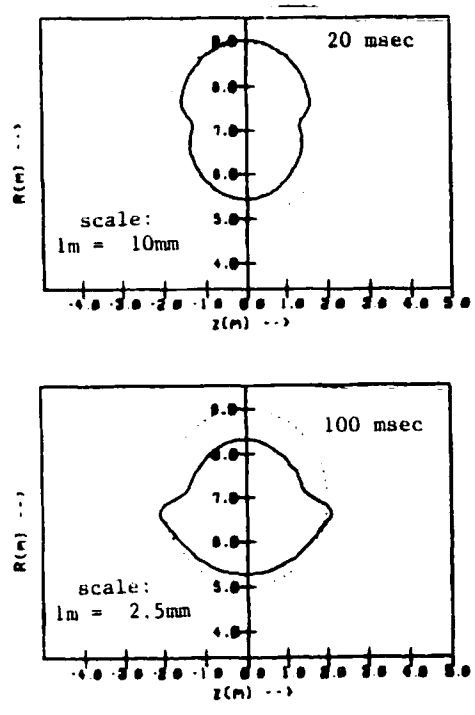

Fig. 6 Base Case Displacements

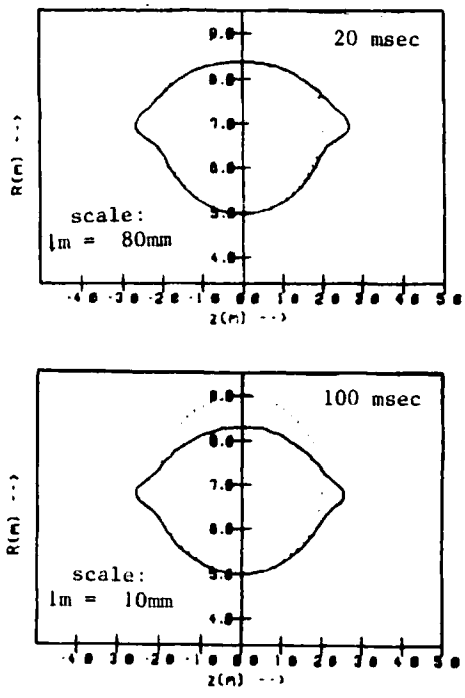

Fig. 7 Shifted Plasma Displacements

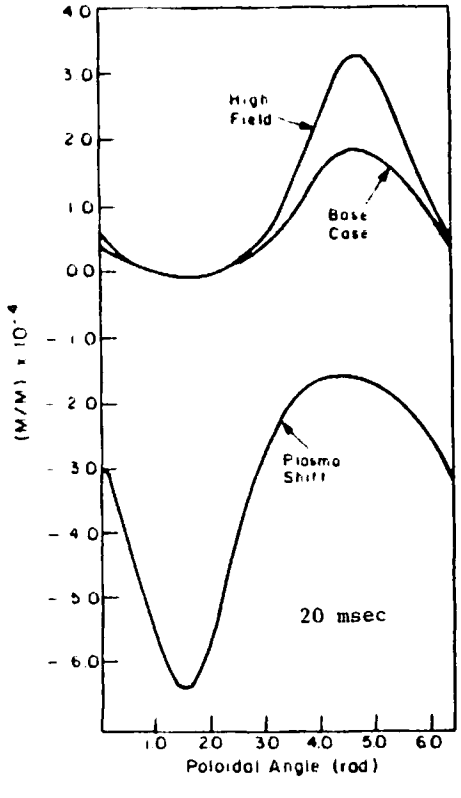

Fig. 8 Toroidal Strains at 20 msec

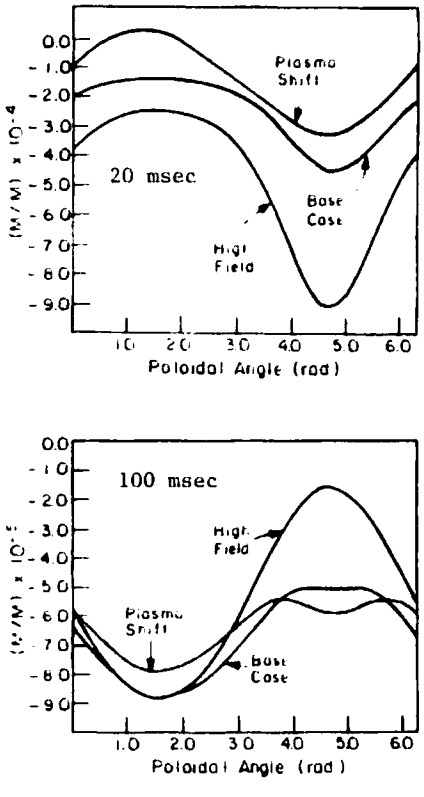

Fig. 9 Poloidal Strains at 20 and 100 msec

describe analytically. In order to explore the range of resonant motions and frequencies, the PAFEC finite element code was employed using an unrestrained thin toroidal shell 1 cm thick with a minor radius of 1 m and an aspect ratio of 3. In a real blanket the type of restraint will dominate the resonant behavior, however it is illustrative to examine the resonant behavior for a simple geometry.

For a toroidal mode number of zero, the frequencies range from 13 Hz to several hundred Hz for poloidal mode numbers of less than about 5. Of course, the frequency range is unbounded on the upper end because mode numbers can be arbitrarily high. However, the greatest strains tend to come from the lower range of mode numbers. In some frequency ranges, the density of resonances exceeds one per Hz. Since the width of the resonances, Q, is likely to exceed a few Hertz, a continuum of resonant behavior may exist over some frequency ranges. The value of Q depends on the materials properties and tends to be larger when nonuniformities and constraints are included. Table 2 lists some of the resonances and their mode numbers. Note, the poloidal mode number does not necessarily correspond to the number of nodal points.

THREE DIMENSIONAL EFFECTS

Enhancement of the stresses and strains over the uniform shell example given above can arise due to nonuniform loading conditions or nonuniform structures. Both of these have been examined in detail using a 3-dimensional method similar to the one described above. A 3-dimensional shell circuit analog eddy current code was used in conjunction with the PAFEC finite element code to explore stress enhancement near a hole and stress enhancement due to plasma current distributions possesing a helical island structure. The induced currents and stress distributions in a 3-dimensional shell are very complicated; therefore the modeling will not be presented here. In the case of a uniform shell with nonuniform plasma current, the results indicate that the ratio of the peak-to-average stress was very nearly the same as the ratio of the peak-to-average induced current. For the case of a shell with a hole in it, the current near the hole rises above the average value slightly, but the stress rises by a factor of 10-15. This effect can be well estimated by traditional methods of calculating stress concentration factors using a simplified estimate for the pressure loading.

Table 2 Resonant Frequencies of a Torus

Mode No. (Tor/Pol)	Frequency (Hz)	Mode No. (Tor/Pol)	Frequency (Hz)
0/2	13.5	1/2	94.9
0/3	128.8	1/3	126.9
0/4	129.4	1/4	129.2
0/5	134.2	1/5	131.8
0/6	137.9	1/6	140.5
0/7	164.6	1/7	162.9
0/8	171.9	1/8	173.4
0/9	185.7	1/9	182.1
0/10	196.6	1/10	198.5
2/1	25.7	2/4	132.5
2/2	56.6	2/5	139.9
2/3	128.5	2/6	148.9

CONCLUSIONS

It is demonstrated that the non-resonant structural response of a uniform toroidal first wall structure is well below the structural limits imposed for ordinary engineering materials. For the STARFIRE-like base case, the radial pressures reach a peak value of 0.35 MPa, and are directed inward toward the plasma throughout the majority of the disruption. Peak poloidal strains of .05% at the inboard edge and bending stresses of 0.7 MPa at the top and bottom are observed.

Reasonable variations in plasma and device parameters resulted in strains which were higher by no more than about a factor of 2. High aspect ratio designs tend to exhibit lower induced strains, whereas compact, low aspect ratio designs have larger strains and poloidal asymmetry. Plasma shift can have a significant influence on both the level of strain and its spatial dependence. The peak bending stress observed with a 25% plasma shift is 10 MPa, with a peak strain of .06% in the toroidal - rather than poloidal - direction.

The existence of structural resonances is likely to enhance the strains by as much as a factor of 10 above the non-resonant values. In addition, discontinuities in the structure and stress concentrations at attachments can contribute a similar enhancement over the uniform structure values. Given that fusion first walls are already designed close to their allowable operating limits, it is clear that disruptions should play a major role in their structural design. Two other important effects of disruptions not treated here include melt layer stability and effects of the high heat and particle loads.

REFERENCES

1. M. S. Tillack, M. S. Kazimi, and L. M. Lidsky, "Aspects of the Structural Effects of Plasma Disruptions on Tokamaks," MIT Dept. of Nuclear Engineering and Plasma Fusion Center, PFC/RR-83-30, 1983.

2. W. Flugge. Stresses in Shells, Springer-Verlag, New York, 1966.